

LARGE-SCALE HYDROTHERMAL ZONING REFLECTED IN THE TETRAHEDRITE-FREIBERGITE SOLID SOLUTION, KENO HILL Ag-Pb-Zn DISTRICT, YUKON

J.V. GREGORY LYNCH*

Department of Geology, The University of Alberta, Edmonton, Alberta T6G 2E3

ABSTRACT

The zoned Keno Hill vein system of central Yukon extends laterally from a Cretaceous plutonic-metamorphic center and surrounding quartz-feldspar veins, to carbonate-Ag-Pb-Zn deposits, and further to peripheral veins having epithermal characteristics. Seven distinct mineralogical zones are recognized, and the entire sequence is continuous from east to west in a 40-km belt. The fault-and fracture-controlled veins are stratabound to the brittle moderately dipping Keno Hill Quartzite unit, of Mississippian age. The unit is graphitic and appears to have acted as a large-scale hydrothermal aquifer, restricting fluid flow during mineralization and development of zoning predominantly to the lateral direction. Tetrahedrite is distributed along a 25-km-long portion of the system, and is the principal ore mineral of Ag. Both Ag/Cu and Fe/Zn values in tetrahedrite are highest at the outer extremity of the system, where freibergite dominates over tetrahedrite; silver-rich samples are also distinguished by an overall increase in the number of cations per formula unit; the Sb/As value is high throughout.

Keywords: hydrothermal zoning, aquifer, tetrahedrite, solid solution, plutonic, epithermal, alteration, Keno Hill district, Yukon.

SOMMAIRE

Le système de veines de la région de Keno Hill, dans la partie centrale du Yukon, est étalé autour d'un centre de plutonisme et de métamorphisme d'âge crétacé, et des fissures à quartz + feldspath associées, et s'étend à des gisements de carbonate-Ag-Pb-Zn et, dans les régions périphériques, à un système de veines à caractère épithermal. Sept zones minéralogiques distinctes sont étalées de façon continue d'est en ouest sur une distance de 40 km. Les veines, dont la distribution est régie par un système de failles et de fissures, sont limitées à la quartzite cassante et à faible pendage de Keno Hill, d'âge mississippien. C'est un encaissant graphitique qui semble avoir agi comme nappe aquifère à grande échelle, canalisant le flux de fluide hydrothermal au cours de la minéralisation dans une direction latérale. La tétraédrite, répandue sur une distance de 25 km dans ce système, est le principal porteur d'argent. Les valeurs Ag/Cu et Fe/Zn de ce minéral sont les plus élevées dans les parties externes du système, où la freibergite est plus répandue que la tétraédrite. Les échantillons riches

en argent se distinguent aussi par une augmentation dans le nombre de cations dans leur formule chimique. Le rapport Sb/As demeure uniformément élevé.

(Traduit par la Rédaction)

Mots-clés: zonation hydrothermale, nappe aquifère, tétraédrite, solution solide, plutonique, épithermal, altération, district de Keno Hill, Yukon.

INTRODUCTION

This paper concerns the large-scale nature of the Keno Hill hydrothermal system. A broad and continuous sequence of mineral zoning can be documented within veins distributed along an extensive portion of the Keno Hill Quartzite, which is the main host rock to the ore in the area. The Keno Hill mining district is located in central Yukon, 350 km north of Whitehorse (Fig. 1). Since 1913, over 4.54×10^6 t ore averaging 1412 g/t Ag, 6.8% Pb, and 4.6% Zn have been mined, and in excess of 6.4×10^9 g of silver have been produced (Watson 1986).

The class of deposit relevant to the Keno Hill veins is referred to by several designations: Cordilleran vein-type deposits (Guilbert & Park 1986), felsic-intrusion-associated silver-lead-zinc veins (Sangster 1984), Pb-Zn sulfide Ag-sulfosalt deposits (Andrews 1986), or polymetallic veins. Despite the considerable economic importance of such veins, relatively little relevant research has been carried out in the last decade (Andrews 1986), and consequently their general characteristics and genesis are poorly understood.

In the most extensive geological work on the veins of the Keno Hill district, Boyle (1965) gave a thorough documentation of the various mineral associations. He recognized separate mineralogically distinct groups of veins throughout the region: cassiterite, wolframite, scheelite and related minerals occur near Cretaceous plutonic bodies, whereas veins containing siderite, galena, sphalerite, and freibergite are separated from the plutons. Boyle considered the two groupings to be unrelated; the silver lodes were thought not to be associated with the plutons, either spatially or genetically (Boyle 1965). Boyle concluded that the metals were emplaced vertically from below through diffusion processes; a flowing

*Present address: Cordilleran Division, Geological Survey of Canada, 100 West Pender Street, Vancouver, British Columbia V6B 1R8.

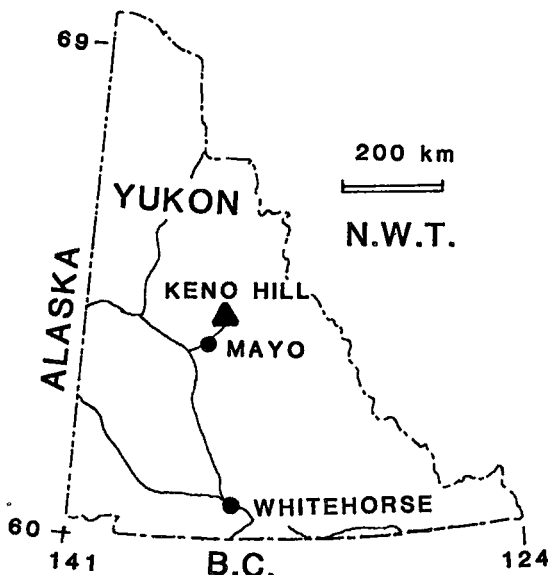


FIG. 1. Location map of Keno Hill mining district in central Yukon.

hydrothermal medium was not favored. However, hydrothermal features are clearly displayed in the vein system. Also, similar Cretaceous ages for the silver veins and for the felsic plutons of the region indicate the possibility of a genetic link (Sinclair *et al.* 1980, Godwin *et al.* 1982).

District-wide mineral zoning within the Keno Hill vein system is documented in this paper. Economic and noneconomic parts of the district are both considered in establishing the continuity of the zones. The patterns indicate a spatial association among the silver deposits, tin mineralization and the Mayo Lake pluton. Lateral movement of evolving hydrothermal fluids during mineralization along fractures in the Keno Hill Quartzite is indicated. The lateral distribution of minerals allows for the exposure of a complete cross-section of the hydrothermal column, at the present level of erosion, from plutonic to epithermal end-members. The documented zoning corresponds to Spurr's (1907, 1912) classic generalized models of zoning.

A quantitative approach to the study of geochemical zoning was pursued through an electron-microprobe investigation of the tetrahedrite-series minerals. Seventy electron-microprobe analyses were performed on tetrahedrite samples from 12 different deposits across the district. Argentian tetrahedrite, the most important silver ore-mineral in the Keno Hill district, occurs throughout a 25-km-long portion of the laterally zoned system. As reported in the literature, tetrahedrite tends to increase in Ag/Cu and Sb/As in the more evolved deposits

(Hackbarth & Petersen 1984); Fe/Zn increases as well in some cases (Jambor & Laflamme 1978). Substitutions are generally insensitive to temperature, but respond to changing chemistry of the fluid (Sack & Loucks 1985). However, in the silver-rich end-member, freibergite, there may be a crystallographic restriction to the amount of arsenic present (Johnson & Burnham 1985). In the Keno Hill area, the compositional changes in tetrahedrite correspond well with the broad mineralogical zones.

Samples were gathered as a result of local surface mapping at various scales, logging of drill cores, and detailed mapping of underground exposures and open pits. X-ray diffraction was used to confirm optical identifications of the ore minerals.

GEOLOGICAL SETTING

The Mississippian Keno Hill Quartzite, which hosts the high-grade silver deposits, outcrops in the Selwyn Basin, in a region that forms the northern extension of the Omineca Belt. The Belt is a collision-related, Cordilleran-scale, plutonic-metamorphic belt overlapping accreted terranes and the North American craton (Tempelman-Kluit 1979, Monger *et al.* 1982).

The quartzite extends for more than 220 km along strike and is bounded above and below by thrust faults (Fig. 2). The strata dip moderately toward the south, and thrusting was generally toward the north. The main unit below the quartzite is the Jurassic "Lower Schist" unit (Poulton & Tempelman-Kluit 1982). Above the quartzite are overthrust "Grit Unit" rocks of the Proterozoic Windermere Supergroup, Siluro-Ordovician Road River Formation, and "Upper Schist" unit rocks of undetermined age. This deformed sedimentary package, metamorphosed to the greenschist facies, is cut by bimodal Cretaceous felsic plutons: an alkaline suite to the west of the district, and a granitic suite in the region near the mining district (Anderson 1987). The sequence of thrusting and pluton emplacement postdates the Jurassic Lower Schist and terminates with Cretaceous plutonism.

The Keno Hill Quartzite is a dark grey, graphitic quartzite with minor muscovite, chlorite, tourmaline, zircon, and usually less than 5% carbonate. Individual layers of quartzite are typically from 1 to 3 m thick and have thin interlayers of graphitic schist. In the area of Keno Hill-Galena Hill, the structural thickness of the quartzite is approximately 1 km. Other than bedding, sedimentary structures are not common. The quartzite has been recrystallized and contains concordant segregations of metamorphic quartz. Finely crystalline grey limestone or marble units are widely distributed but are not abundant.

Concordant lenses of "greenstone" are abundant throughout the Lower Schist and in the Keno Hill

Quartzite, but are less abundant in the Upper Schist. The lenses are 1 m to 30 m in thickness, and locally persist along strike for more than 1 km. They are interpreted to be the metamorphosed equivalents of gabbro and diorite sills (Green 1971). Their most

common metamorphic assemblage is zoisite–albite–actinolite–chlorite ± stilpnomelane (McTaggart 1960). The lenses are older than the undeformed granitic bodies (mid-Cretaceous), and possibly were cogenetic or younger than the Jurassic rocks.

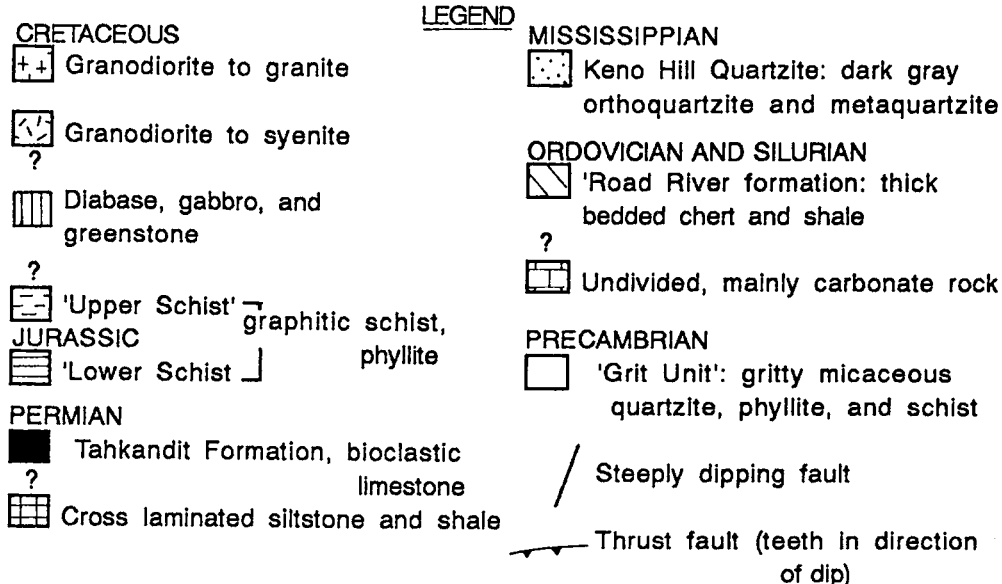
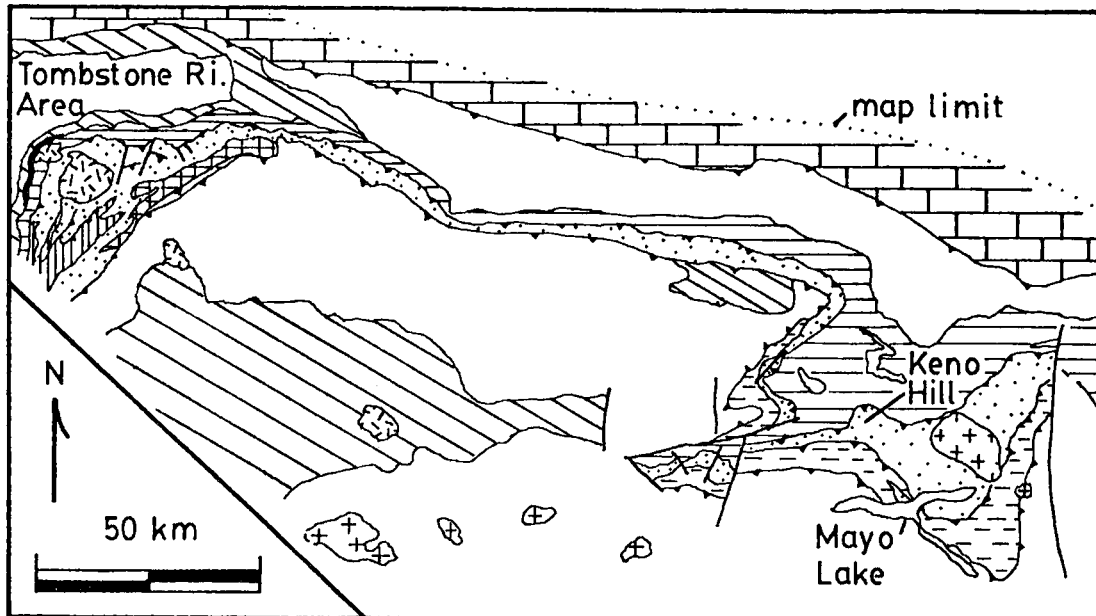


FIG. 2. Geological map of region surrounding Keno Hill, and Keno Hill Quartzite (modified from Tempelman-Kluit 1970).

The Mayo Lake pluton cuts the Keno Hill Quartzite to the east of the mining district (Fig. 3). It has been dated by the K-Ar method at 81 Ma (GSC map 1398A). The pluton varies from a core of coarse porphyritic granite containing megacrysts of alkali feld-

spar, black amphibole, and minor titanite, to a margin of finer equigranular granodiorite with green amphibole. Contact metamorphism extends outward for up to 4 km. Sillimanite schist at the contact grades outward into garnet-staurolite-feldspar

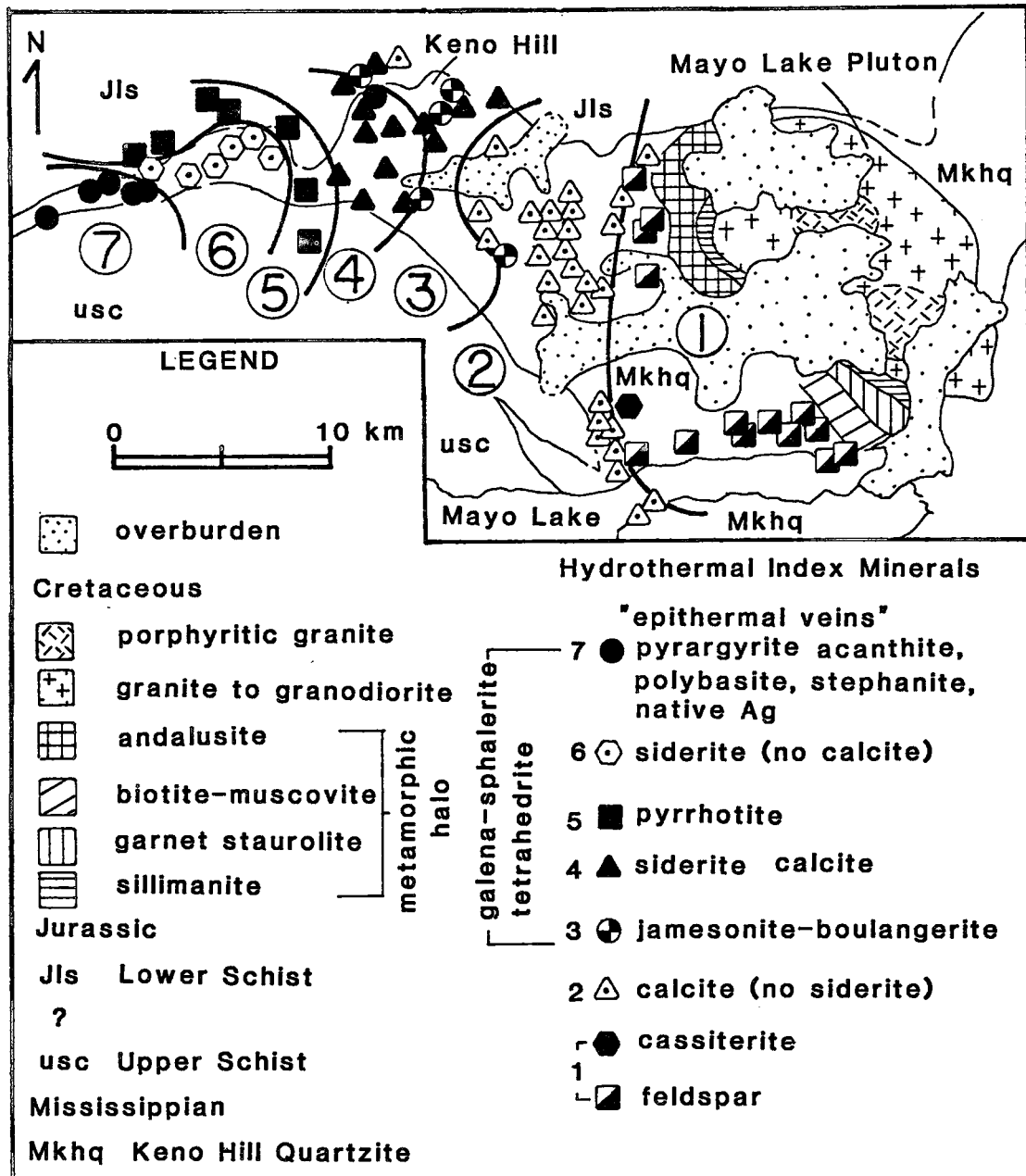


FIG. 3. Map of principal zones of hydrothermal minerals within the Keno Hill district, and relation of veins to the Mayo Lake pluton in the eastern portion of the map. The diagram emphasizes mineralogical differences, though there is considerable overlap between zones.

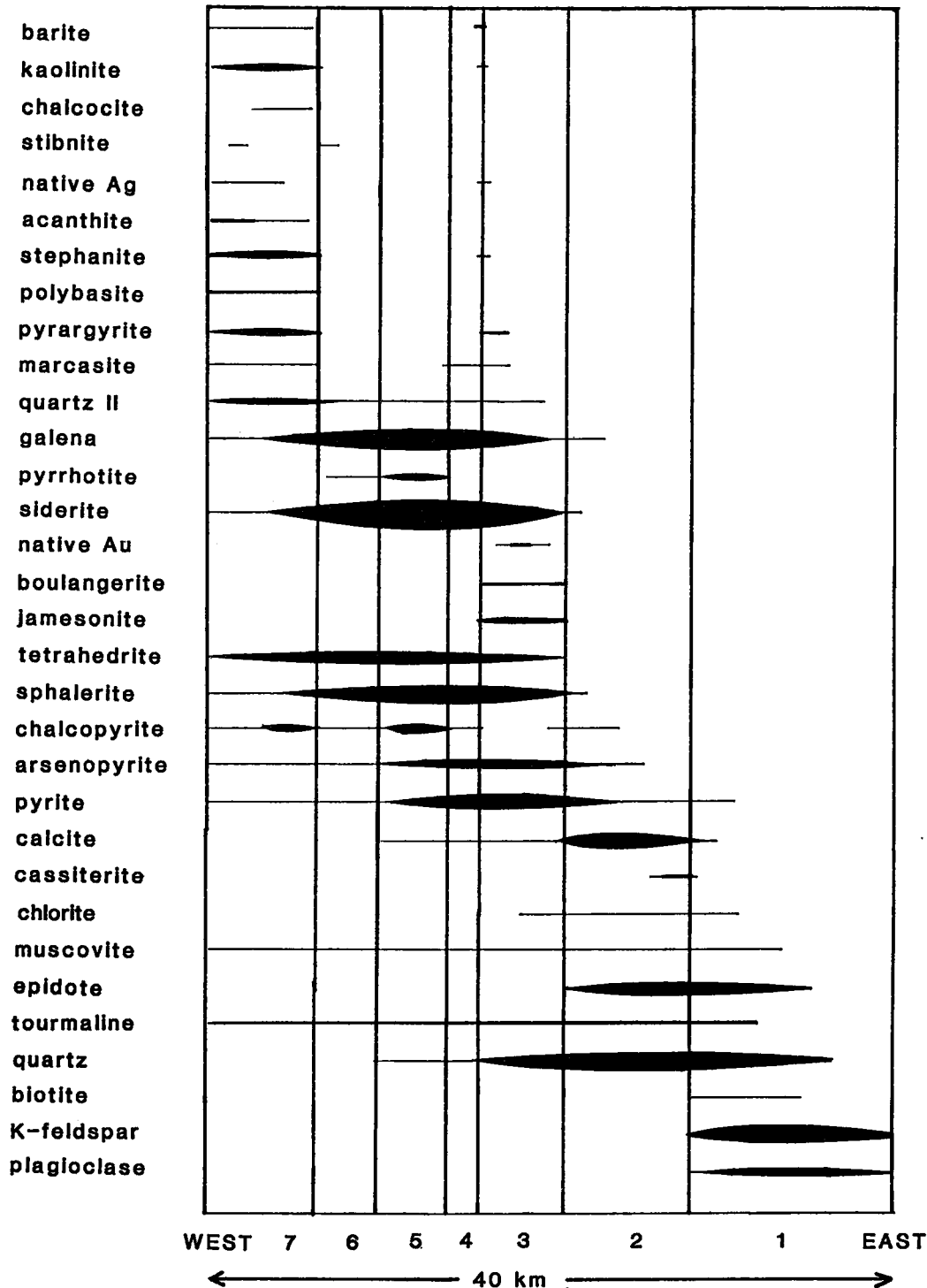


FIG. 4. Bar diagram of east-to-west mineralogical zoning, which displays mineralogical overlap between zones. The thickness of bars gives a schematic representation of relative abundance.

schist. The most distal part of the aureole is characterized by biotite-muscovite schist at low altitudes (700–1220 m) and graphite-andalusite schist at higher

altitudes (1525–1825 m). Texturally, the andalusite crystals have a variable orientation within the schist and overgrew deformation fabrics. Pressure shadows

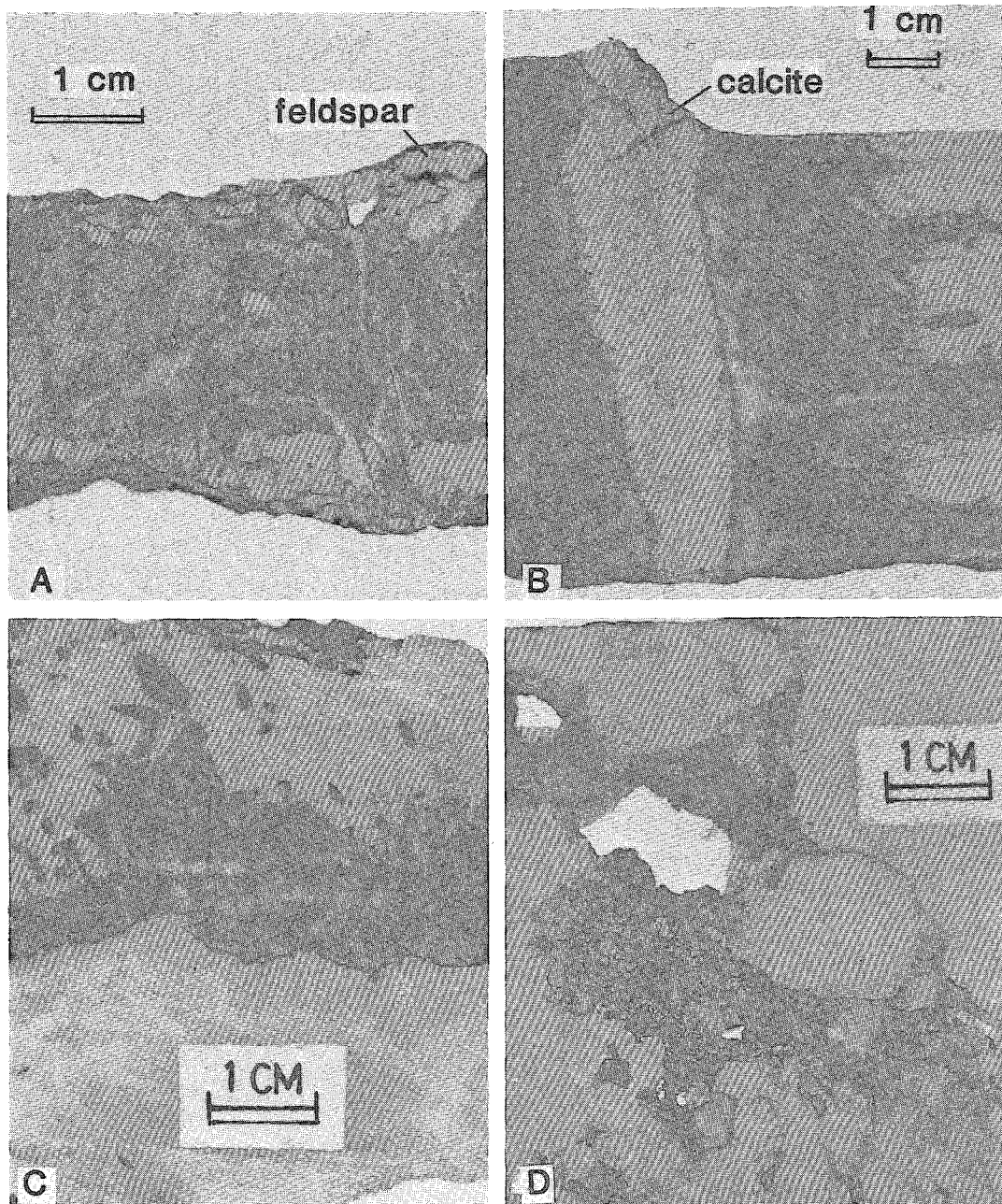


FIG. 5. Veins east of the mining district near the Mayo Lake pluton; (A) banded quartz-feldspar vein displaying euhedral light-colored feldspar along the upper and lower vein margins; (B) quartz-calcite vein with carbonatization halo in sericitic quartzite; (C) banded calcite and calcite-epidote vein from near margin between calcite zone and feldspar zone; (D) photograph displays coarse vuggy nature of quartz veins, with some interstitial galena.

were not found around garnet crystals. Such features indicate a predominantly post-kinematic age for the final emplacement of the Mayo Lake pluton. Green-

stone lenses near the pluton have been converted to hornblendite. A tungsten skarn is reported to occur along the western contact of the pluton (Bostock

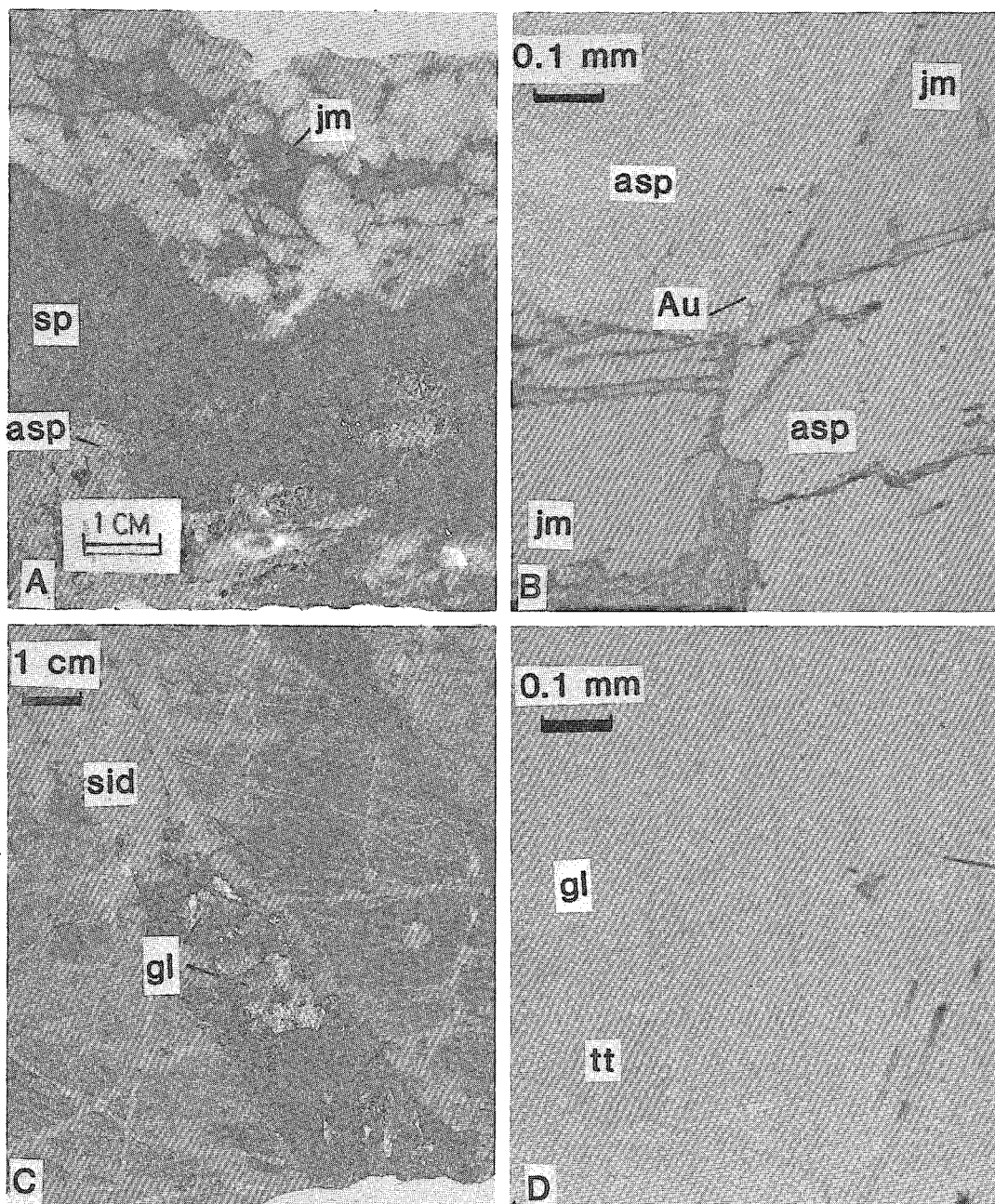


FIG. 6. Veins from the mining district and central portion of hydrothermal system; (A) banded vein with massive arsenopyrite (asp), and sphalerite (sp) along vein margin, with quartz (white) and jamesonite (jm) toward the vein center; (B) photomicrograph showing position of native gold (Au) between arsenopyrite (asp) and jamesonite (jm) crystals; (C) typical galena (gl)-pyrite-siderite (sid) vein cross-cutting early quartz stockwork in dark graphitic quartzite host; (D) micrograph of tetrahedrite (tt) inclusions in galena (gl).

1948), but that remote showing was not visited during the course of this study.

Aplite and pegmatite dykes are common along the margins of the pluton. Quartz-feldspar porphyry

dykes, locally with amphibole, extend over a broad area (Boyle 1965) but are not abundant. They have been dated at 81 ± 5 Ma (Green 1971). Rare lamprophyre dykes of undetermined age also occur in

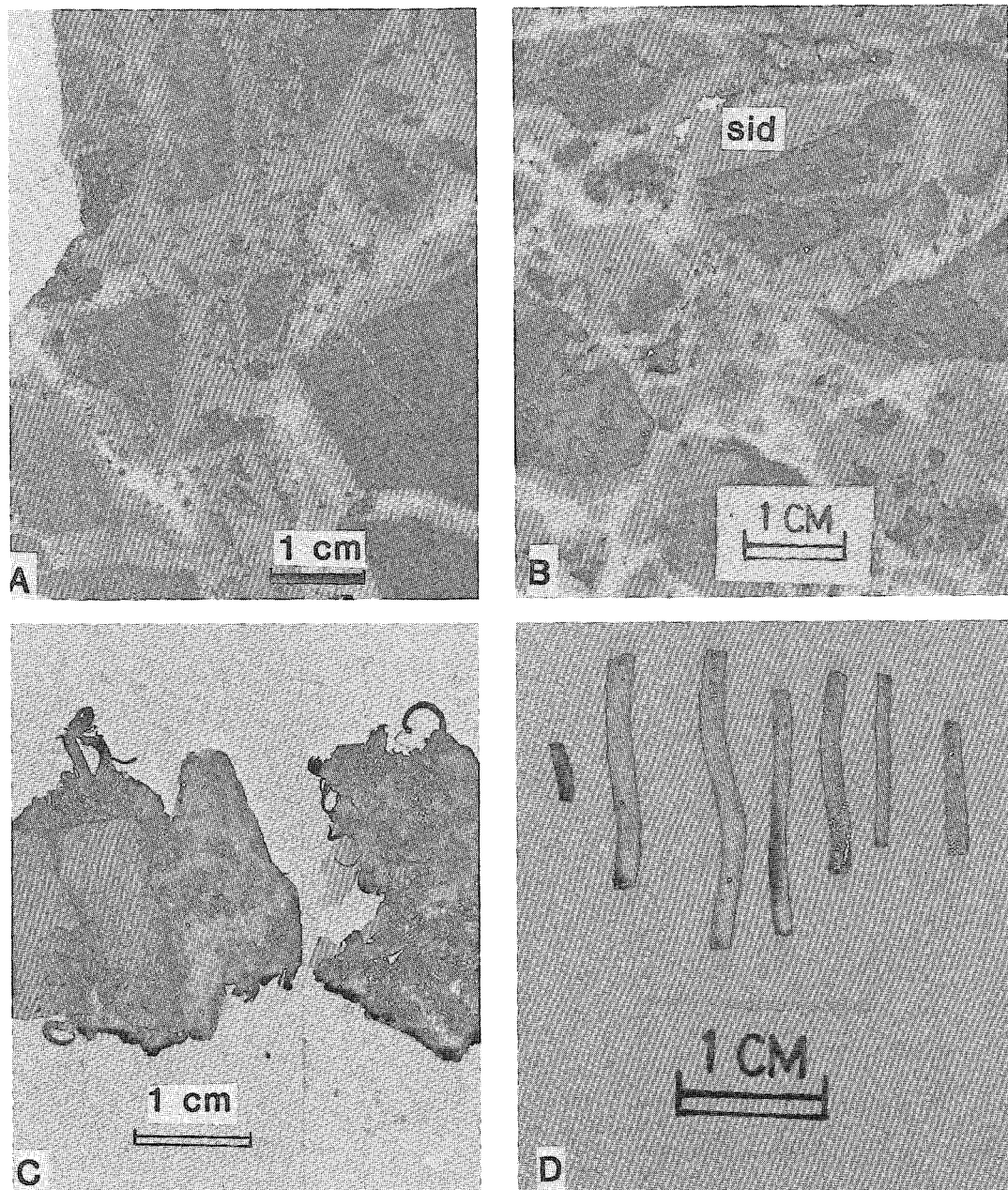


FIG. 7. Veins from western epithermal system; (A) breccia of dark graphitic quartzite clasts cemented by siderite (light color) and overgrown by quartz (white) with fine-grained dark pyrargyrite; (B) subrounded breccia clasts of quartzite (dark) and hydrothermal siderite (light-colored), cemented by the late hydrothermal quartz stage (white); (C) coarse wire silver; (D) hollow and spiralling tubes of pyrite.

the district. Micas from hydrothermal alteration surrounding the Ag-Pb-Zn veins of the mining district have been dated (K-Ar) to be mid-Cretaceous (84 ± 4 Ma; Sinclair *et al.* 1980), which shows that they are contemporaneous with the felsic intrusive bodies.

HYDROTHERMAL VEINS AND MINERAL ZONING

Hydrothermal veins are widespread within the Keno Hill quartzite. The frequency of the veins is variable from outcrop to outcrop; commonly, only one or two veins are found in an exposure. Nevertheless, the veins are distributed across tens of kilometers, and collectively form a close, complicated network on a larger scale.

Hydrothermal veins of the mineralizing event usually can readily be distinguished from the earlier segregations of metamorphic quartz formed during the greenschist metamorphic event. Hydrothermal veins are coarse grained, vuggy, with euhedral to subhedral crystals, display strong banding textures, are structurally discordant and locally have a well-developed alteration halo. Segregations of metamorphic quartz are concordant, finer grained, massive, usually monomineralic, and exhibit strain features.

Structural control of veins was considered by McTaggart (1960), Boyle (1965), and Lynch (1989). The orebodies are contained within an extensive set of sinistral, strike-slip and dip-slip faults, which strike northeast and dip steeply to the southeast. Much of the vein material is unstrained, but parts of some veins contain sheared and deformed crystals; brecciated hydrothermal vein minerals are cemented by later hydrothermal minerals, indicating that faulting and hydrothermal activity could have been contemporaneous. Two other types of fractures are important in localizing veins: 1) widespread north- to northeast-striking "AC" tension fractures, and 2) north- to northwest-striking fractures. Both sets dip steeply.

Within the system, adjacent veins and deposits have characteristic mineral assemblages that distinguish them from veins in other parts of the district; these form mineralogical zones distributed along the length of the hydrothermal system (Figs. 3, 4). Adjacent zones are identified by the appearance or disappearance of specific index minerals, and characteristic assemblages of minerals. Other minerals that overlap between zones (*e.g.*, epidote is found in both of the adjacent feldspar and calcite zones) demonstrate the continuity of the vein system.

The veins are texturally quite variable along the length of the belt. Quartz crystals in the region proximal to the pluton are euhedral and up to 20 cm long, and display a comb texture. Cross-cutting relations are not complex in this area, though layering within the veins or banded texture is commonly seen (Fig.

5). In the distal region, euhedral quartz crystals are commonly less than 5 mm long, and cross-cutting relations of the various sets of veins are considerably more complex. Various types of stockworks and breccias are observed (Figs. 5A, B, C). A vuggy texture in the veins, indicative of open-space filling, is characteristic of the entire system from east to west.

Figures 3 and 4 illustrate the mineralogical zoning that is described below.

Feldspar zone

The presence of feldspar in the veins marks the innermost hydrothermal zone around the Mayo Lake pluton. Both potassium feldspar and plagioclase are found. Rock staining and thin section petrography were useful in distinguishing the two. Locally, the potassium feldspar has a perthitic texture, and in some cases a tarten twinning, indicating the presence of microcline. Plagioclase ranges in composition from albite to labradorite. Occasionally feldspar forms vermicular intergrowths with quartz.

Many of the feldspar-bearing veins have euhedral yellowish feldspar dominating the vein-wallrock contact, and quartz in the center of the vein (Fig. 5A). Minor constituents include zoisite, pyrite, apatite, tourmaline, and rare ilmenite. The alteration of the quartzite is typically weak and may include a small inner halo of feldspathization, with outward sericitization. The alteration of greenstones is more complex: chlorite and combinations of anthophyllite, clinozoisite, and fine-grained actinolite are typically abundant; also present is a weak alteration containing potassium feldspar and plagioclase near the vein and biotite farther out. The original plagioclase in the greenstones appears unaltered. A late stage of microscopic calcite and siderite fills cracks and microveinlets that cut through earlier vein material.

Cassiterite in quartz veins is uncommon, but serves as a useful index mineral for the near-plutonic environment. The cassiterite-bearing veins occur near the outer margin of the feldspar zone, almost 10 km from the pluton (Fig. 3). Coarse flakes and books of muscovite occur along the margins of some of these vuggy quartz veins. Other minerals are rare in these veins, but include pyrite and arsenopyrite. Alteration haloes involve moderate sericitization of the host. It may be significant that the galena of the mining district is reported to have a high tin content (Boyle 1965), a further link between the cassiterite-bearing veins and the Ag-Pb-Zn orebodies.

Calcite zone

The presence of calcite marks a broad and distinct zone between the silver-rich veins of the mining district to the west and the feldspar-bearing veins in the vicinity of the pluton. Coarse calcite in variable

abundances is the most distinguishing feature of this zone (Fig. 5B). Euhedral zoisite and epidote commonly occur with the calcite (Fig. 5C), and are important overlap minerals between the feldspar zone and the carbonate zone. Small amounts of pyrite, arsenopyrite and chalcopyrite are usually found in these veins. Multiple banding or layering is a common texture in the veins (Fig. 5C). Albite intergrown with calcite and quartz was observed in a few samples from near the eastern feldspar zone. The degree of host-rock alteration is more pronounced in the calcite zone, and the appearance of sulfides is more widespread. Carbonatization and sericitization haloes surround the veins in the quartzite, and have a marked bleaching effect due to graphite removal. Chlorite, epidote, carbonate and sericite haloes are more abundant where the greenstone is the host unit. Although these veins have mineralogical features resembling mesothermal precious-metal deposits, they have not been extensively explored, and their economic potential is uncertain.

Jamesonite–boulangerite zone

The overall mineralogical changes within this zone are considerable. A characteristic feature is the appearance of bladed, medium-grained crystals of jamesonite and boulangerite. The presence of both minerals in this mining district was established by Boyle (1965); they commonly occur together, but jamesonite appears to be more abundant. Beginning with the jamesonite–boulangerite zone, the overall abundance of opaque minerals in the veins rises sharply (Fig. 6A). The opaque phases include arsenopyrite, pyrite, chalcopyrite, light brown sphalerite, tetrahedrite and traces of fine-grained native gold (Fig. 6B). Cross-cutting relations increase in complexity in this zone. Thick sphalerite-rich layers alternate with arsenopyrite, pyrite and tetrahedrite layers. Pure quartz zones also occur. Many large euhedral quartz crystals have been brecciated and cemented by felted masses of jamesonite–boulangerite, indicating forceful hydrothermal activity or contemporaneous fault movement. Portions of the veins contain only quartz and calcite with minor pyrite, and are similar to the veins of the previous zone.

Gold is typically microscopic and occurs along the margins of arsenopyrite crystals or with pyrite and tetrahedrite. Placer operations are active in the vicinity of these veins, which are considered the source of the placer gold.

Siderite

Siderite, the most widespread and characteristic gangue mineral within the silver orebodies, occurs

with pyrite, galena, sphalerite and tetrahedrite. On Keno Hill, this assemblage is intergrown with quartz, arsenopyrite and calcite. However, arsenopyrite and calcite are less abundant or, more typically, absent in veins to the west, on Galena Hill, allowing for the siderite zone to be further subdivided (Fig. 3). Texturally, the siderite is coarse to medium grained and massive. It cements breccias and fills stockworks in fault structures. In the upper parts of some veins it is oxidized to iron and manganese hydroxides.

Wallrock alteration is characterized by sericitization with pyrite and minor tourmaline, as well as carbonatization. A more chlorite-rich assemblage typifies the alteration of the greenstone lenses.

Siderite does not generally occur with jamesonite and boulangerite, but is found along strike in some of the same fault structures. Jamesonite and boulangerite also appear in splay faults connecting directly to the main siderite-bearing veins. In some localities, siderite veins cut jamesonite–boulangerite–quartz veins (Fig. 6C). The overlap between these two groups is observed only on Keno Hill.

Pyrrhotite zone

Pyrrhotite occurs as an accessory mineral in several of the deeper veins exposed in the low-lying area between Galena Hill and Keno Hill (Fig. 3). In two of the deposits, Duncan Creek and Flame-Moth veins, it is more abundant. Below 900 m in altitude, siderite–pyrite–galena–sphalerite–tetrahedrite veins may contain calcite, arsenopyrite and pyrrhotite as well. However, these three minerals disappear at higher elevations on Galena Hill and to the west at low elevations beyond Galena Hill. This is the only clearly established mineral zonation with a distinct vertical component in the district. Most of the other zones adjoin laterally because diagnostic minerals are found at various altitudes. As a group, pyrrhotite-bearing veins form a narrow belt that closely follows contours along the western flank of Galena Hill (Fig. 3).

Pyrrhotite is replaced by marcasite along partings in crystals, fractures in aggregates and along grain boundaries. Fresh samples of pyrrhotite commonly have extensive graphic intergrowths with sphalerite. The sphalerite may also show evidence of "chalcopyrite disease".

Pyrargyrite zone and veins of "epithermal" character

Pyrargyrite is widespread and contributes significantly to the silver values of the western deposits. However, appreciable amounts of the mineral occur in the Lucky Queen mine on Keno Hill in the east (localities of the mines are shown in Fig. 9). The western zone marks the last stage of the system. It

TABLE 1. TETRAHEDRITE COMPOSITIONS, KENO HILL DISTRICT*

	Cu	Ag	Fe	Zn	Cd	Tc	Sb	As	S	TOTAL		Cu	Ag	Fe	Zn	Cd	Tc	Sb	As	S	TOTAL	
Homestake 1	27.21	15.90	3.65	3.20	0.21	0.00	26.70	0.81	21.95	99.65	Lucky-Q 1	18.93	27.09	3.71	2.57	0.88	0.00	25.63	0.82	20.33	99.95	
Homestake 2	26.23	16.41	3.59	3.27	0.23	0.00	26.68	0.78	21.82	99.02	Lucky-Q 1r	19.86	26.50	3.75	2.39	0.97	0.00	25.76	0.84	20.39	100.46	
Homestake 2r	26.07	16.64	3.35	3.33	0.23	0.00	26.94	0.85	21.81	99.12	Lucky-Q 2	15.86	32.85	4.62	1.51	0.64	0.02	25.64	0.76	19.45	101.33	
Homestake 3	26.46	15.59	3.81	3.02	0.19	0.00	26.46	0.77	22.13	98.41	Lucky-Q 3	16.98	30.66	1.38	5.52	0.53	0.00	25.55	0.74	19.52	100.88	
Homestake 4	27.24	15.51	3.74	3.15	0.21	0.00	26.41	0.75	22.04	99.06	Lucky-Q 4	16.62	30.45	3.12	3.24	0.80	0.00	25.05	0.83	19.47	99.58	
Homestake 4r	26.81	15.80	3.49	3.18	0.18	0.00	26.52	0.72	21.93	98.62	Lucky-Q 5	17.07	30.13	1.45	5.54	0.57	0.00	25.21	0.77	19.62	100.37	
Homestake 5	27.37	15.67	3.63	3.68	0.16	0.00	26.41	1.35	22.13	100.42	average	17.55	29.61	3.01	3.46	0.73	0.00	25.47	0.79	19.80		
	average	26.77	15.93	3.61	3.26	0.20	0.00	26.59	0.86	21.97		Ruby 1	16.69	28.74	3.30	2.87	0.28	0.00	26.03	0.32	19.54	97.77
Onek 1	24.84	19.29	4.71	1.86	0.22	0.01	26.72	0.77	21.12	99.53	Ruby 2	16.70	28.99	3.42	2.77	0.20	0.00	25.79	0.31	19.33	97.52	
Onek 1r	25.26	18.93	4.35	2.09	0.22	0.00	26.61	0.78	21.09	99.33	Ruby 4	13.64	34.09	5.74	0.21	0.24	0.00	25.76	0.31	18.39	98.39	
Onek 2	24.68	19.32	4.17	2.45	0.22	0.00	26.41	0.93	21.69	99.88	average	15.68	30.61	4.15	1.95	0.24	0.00	25.86	0.31	19.09		
Onek 2r	24.80	19.00	4.31	2.26	0.20	0.00	26.64	0.83	21.76	99.88	H-R224-A 1	13.45	33.77	4.40	4.15	0.15	0.00	23.95	0.28	19.16	99.31	
Onek 3	23.99	19.04	4.29	2.35	0.23	0.00	26.70	0.75	21.91	99.31	H-R224-A 2	17.04	31.09	4.76	1.48	0.09	0.00	26.33	0.52	19.54	100.87	
Onek 4	24.99	19.27	4.28	2.37	0.23	0.01	26.73	0.70	22.05	100.64	H-R224-A 2r	17.47	29.85	4.73	1.34	0.05	0.00	26.02	0.34	19.33	99.14	
Onek-B 3	23.91	19.13	4.50	1.66	0.15	0.03	27.19	0.55	22.11	99.24	H-R224-A 3	15.30	32.54	3.35	2.65	0.18	0.00	25.61	0.32	18.62	98.77	
Onek-B 3r	23.82	19.33	4.53	1.66	0.13	0.07	27.27	0.58	22.24	99.64	H-R224-A 4	15.75	32.37	4.47	1.56	0.02	0.00	25.56	0.50	19.03	99.26	
average	24.54	19.16	4.39	2.09	0.20	0.03	26.78	0.74	21.75		H-R224-A 4r	14.78	33.40	4.11	2.07	0.06	0.00	25.49	0.36	18.95	99.23	
Sadic 1	19.86	25.00	4.42	1.57	0.25	0.01	26.61	0.15	21.20	99.06	H-R224-B 1	13.78	35.12	4.59	1.56	0.32	0.02	25.23	0.77	17.81	100.09	
Sadic 2	19.23	27.10	4.63	1.42	0.32	0.09	26.26	0.16	21.11	100.31	H-R224-B 2	13.69	35.46	4.75	1.37	0.32	0.01	24.79	1.07	18.66	100.13	
Sadic 3	19.61	27.05	4.65	1.37	0.27	0.09	26.54	0.16	21.11	100.85	H-R224-B 3	12.92	35.46	4.65	1.32	0.38	0.03	24.82	0.73	18.49	98.79	
Sadic 4	19.95	26.21	4.62	1.42	0.23	0.08	26.61	0.15	21.19	100.45	H-R224-B 4	14.90	34.12	4.84	1.29	0.37	0.03	25.33	0.75	18.84	100.47	
Sadic 5	20.03	26.76	4.22	1.88	0.27	0.07	26.29	0.16	21.14	100.81	H-R224-B 5	13.69	34.70	4.67	1.43	0.35	0.01	24.35	0.85	18.61	98.68	
average	19.74	26.42	4.51	1.53	0.27	0.08	26.46	0.16	21.15		average	14.80	33.44	4.50	1.84	0.21	0.01	25.23	0.60	18.90		
Dixie 1	13.50	35.22	4.07	1.71	0.50	0.11	25.87	0.13	18.75	99.87	Husky 1	20.40	24.90	6.25	0.18	0.37	0.00	25.51	0.76	20.59	98.96	
Dixie 2	13.89	35.27	2.20	4.16	0.59	0.14	25.65	0.12	18.74	100.76	Husky 2	16.59	30.13	5.97	0.36	0.37	0.00	25.36	0.73	19.34	98.84	
Dixie 2r	14.20	34.37	3.57	2.37	0.58	0.11	25.93	0.13	18.83	100.10	Husky 3	20.69	24.63	5.51	0.37	0.43	0.00	25.49	0.84	20.61	98.58	
Dixie 3	15.10	33.74	4.36	1.26	0.57	0.12	25.89	0.14	18.94	100.11	Husky 3r	20.37	24.55	5.46	0.41	0.40	0.00	25.45	0.75	20.58	97.97	
Dixie 4	15.39	32.30	5.35	0.48	0.61	0.11	25.63	0.13	19.66	99.67	average	19.51	26.05	5.80	0.33	0.39	0.00	25.45	0.77	20.28		
average	14.42	34.18	3.91	2.00	0.57	0.12	25.79	0.13	18.98		Shamrock 1	19.82	24.95	3.57	4.28	0.52	0.03	26.87	0.12	21.21	101.36	
Silver King 1	14.57	33.86	4.11	2.37	0.38	0.05	25.47	0.78	19.12	100.69	Shamrock 2	19.99	24.91	3.22	3.74	0.56	0.00	26.94	0.13	20.88	100.39	
Silver King 2	14.24	34.94	4.15	2.21	0.40	0.05	25.36	0.81	18.80	100.96	Shamrock 3	18.23	28.35	3.50	3.21	0.44	0.09	26.88	0.12	20.45	101.26	
Silver King 3	13.38	36.35	4.88	1.47	0.39	0.04	25.06	0.70	18.79	101.05	Shamrock 3r	17.27	29.92	3.43	3.11	0.43	0.08	26.63	0.13	20.00	100.98	
Silver King 4	13.15	36.91	4.34	1.97	0.43	0.06	24.70	0.76	18.47	100.79	average	18.83	27.03	3.43	3.59	0.49	0.05	26.83	0.13	20.64		
Silver King 5	14.87	33.95	4.04	2.43	0.37	0.09	25.07	0.74	18.96	100.54												
average	14.04	35.20	4.30	2.09	0.39	0.06	25.13	0.76	18.83		Calumet-A 1	19.69	27.74	3.36	2.17	0.47	0.05	24.55	0.51	20.63	99.16	
											Calumet-A 2	14.89	32.26	2.20	3.99	0.40	0.12	25.86	0.43	18.31	98.45	
											Calumet-B 1	20.20	27.12	3.45	2.52	0.57	0.00	23.91	0.79	19.61	98.18	
											Calumet-B 1r	20.26	26.81	3.53	2.50	0.55	0.00	24.44	0.81	20.51	99.41	
											Calumet-B 2	20.82	24.60	3.43	2.76	0.53	0.00	25.37	0.73	20.15	98.40	
											Calumet-B 3	21.02	23.72	3.65	2.86	0.68	0.00	26.29	0.70	20.50	99.41	
											Calumet-B 4	20.67	24.57	3.55	3.01	0.63	0.00	26.09	0.73	20.32	99.48	
											average	19.65	26.69	3.31	2.83	0.55	0.02	25.22	0.67	20.00		
Porcupine 1	19.53	26.01	1.22	5.45	0.41	0.00	25.95	0.37	20.17	99.07	Porcupine 2	18.62	25.49	3.37	4.03	0.26	0.00	25.88	0.32	20.50	98.47	
Porcupine 2	17.78	28.62	1.03	5.84	0.33	0.00	25.64	0.52	19.76	99.50	Porcupine 3	17.24	28.83	1.35	5.28	0.52	0.00	25.15	0.77	19.81	98.95	
Porcupine 3	18.79	27.77	1.40	5.15	0.57	0.00	26.08	0.66	19.99	100.41	Porcupine 4	18.79	27.77	1.40	5.15	0.57	0.00	25.74	0.53	20.05		
Porcupine 4	average	18.39	27.34	1.67	5.15	0.42	0.00	25.74	0.53													

*Compositions were determined using an electron microprobe, and are expressed in wt. %.

is characterized by other phases as well, which have a more erratic distribution within the zone; these include acanthite, native silver, polybasite, stephanite, stibnite, marcasite, barite, dendritic quartz and kaolinite as an alteration mineral. Such minerals give the deposits a distinctly epithermal character.

Some of the pyrargyrite occurs with galena, freibergite, pyrite, sphalerite, and siderite, but most is intergrown with a late-stage quartz that encrusts vugs in siderite, or in stockwork stringers that cut siderite (Figs. 7A, B). The quartz occurs mainly as fine-grained, euhedral, clear crystals, or as radiating bundles of fine-grained, milky white dendrites. The latter show feather-like skeletal patterns in thin section.

At the Husky mine, a peculiar form of pyrite can occasionally be seen in the veins. Slender tubes of pyrite project into open vugs (Fig. 7C). The tubes are up to 10 cm long and 1 cm in diameter. All are hollow, and give the appearance of having formed as "chimneys" for hydrothermal fluids that seeped

into vugs. Vugs also contain coarse world-class specimens of polybasite and stephanite.

Gersdorffite was detected by X-ray diffraction in one sample, with quartz and siderite. This assemblage occurs with marcasite, chalcopyrite and tetrahedrite rimmed by chalcocite. Minor fine-grained sphalerite also is present. Banded textures show that

the siderite-bearing assemblage is typically overgrown by quartz and pyrargyrite, in turn overgrown by cubes of pyrite. Kaolinite fills some of the vugs.

Host-rock alteration includes recrystallization of the quartzite to a fine-grained granular mass, within intense stockworks of fine quartz veinlets that are densely interwoven and generally not perceptible until the rock has been cut or a thin section made. Sericitization is widespread, as is minor tourmalinization. Kaolinite occurs locally as an alteration mineral, generally with disseminated pyrite. Carbonates are not seen in most alteration haloes. Graphite has been removed in altered sections of host rocks, giving the rock a distinct bleached appearance. Coarse barite is occasionally found and appears as a late-stage mineral that locally cements brecciated fragments of galena and siderite.

Pyrargyrite also occurs separately with acanthite, coarse wires of native silver and fine-grained euhedral quartz (Fig. 7D). This assemblage is well developed in portions of the Silver King mine.

It was not clearly established in the past whether pyrargyrite and some of its associated minerals are of supergene or hypogene origin (Boyle 1965). The present interpretation is that minerals of this suite are mainly of hypogene origin. In new mine workings of the Husky orebody, much of the pyrargyrite is associated with pyrite cubes and quartz crystals; the pyrite is fresh, and crystallized quartz does not generally form as a result low-temperature supergene processes. Also, pyrargyrite in nature is more commonly observed as a hypogene rather than a supergene mineral in vein systems (Guilbert & Park 1986).

TETRAHEDRITE CHEMISTRY

Analytical methods

Electron-microprobe analyses of tetrahedrite samples were performed at the Department of Geology, the University of Alberta, using an ARL-SEMQ microprobe. Quantitative wavelength-dispersion analyses (WDS) were done at 15 kV operating voltage, 4 nA probe current and 100 s counting time. Data were processed with full-matrix (ZAF) corrections using EDATA2 (Smith & Gold 1979).

Concentrations of nine elements (Cu, Ag, As, Sb, Fe, Te, Cd, Zn, and S) were determined at each point. Pure metal standards were used for each element, except that marcasite and arsenopyrite were used for Fe and As. All analytical totals range between 97 and 101 wt.-%.

Analytical results

Texturally, tetrahedrite occurs predominantly as round, bleb-like inclusions, typically < 0.1 mm in diameter, in coarser-grained galena (Fig. 6D). A multitude of these inclusions may be contained within a single crystal of galena. Tetrahedrite in this form was analyzed from the various deposits of the district to maintain sample consistency. Except for the sheared galena from the Calumet and Shamrock mines, galena used in the microprobe study shows little sign of strain.

Microprobe data are summarized in Tables 1 and 2. The tetrahedrite chemistry approximates the following stoichiometry (Sack & Loucks 1985): $\text{TRG}(\text{Cu}, \text{Ag})_6^{\text{TET}}[\text{Cu}_{\frac{1}{3}}(\text{Fe}, \text{Zn}, \text{Cd}, \text{Hg}, \text{Pb})_{\frac{1}{3}}]_6^{\text{SM}}(\text{Sb}, \text{As}, \text{Bi})_4^{\text{OCT}}(\text{S}, \text{Se})_{13}$, where the symbols TRG, TET, SM, and OCT stand for trigonal planar, tetrahedral, semimetal, and octahedral sites, respectively. The semimetals are typically divided among three tetrahedral sites and one trigonal planar site (Johnson *et al.* 1988). However, considerable departures from this ideal formula are widely reported in the literature, particularly in the case of Ag-bearing tetrahedrite (Johnson *et al.* 1986). Discrepancies are observed in both naturally occurring and synthetic

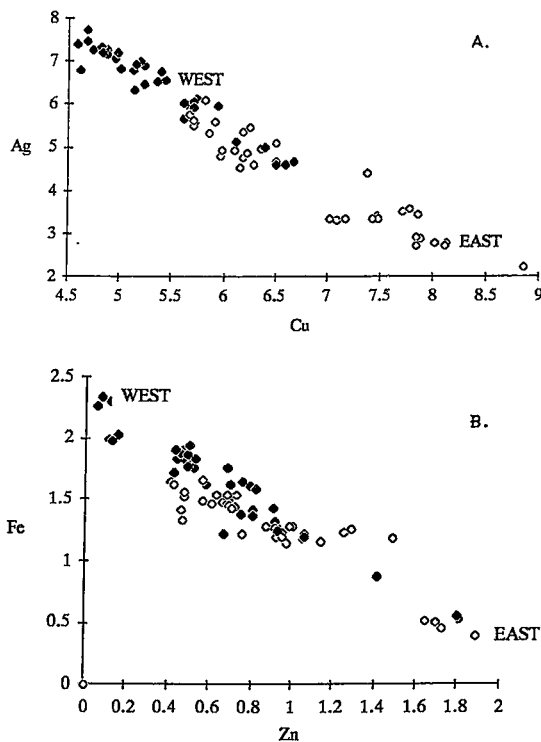


FIG. 8. (A) Negative linear relation between silver and copper proportions in the tetrahedrite-series minerals. (B) Negative linear relation between iron and zinc proportions in the tetrahedrite-series minerals. Filled pattern: samples from western portion of the district; open symbols: samples from the east. Values are quoted in number of atoms relative to 13 atoms of sulfur.

tetrahedrite (Makovicky & Skinner 1978). In some cases, Ag-depleted tetrahedrite does not correspond to the formula as well; Skinner *et al.* (1972) synthesized tetrahedrite with the composition $\text{Cu}_{12+x}\text{Sb}_{4+y}\text{S}_{13}$, where $X \leq 1.9$ and $Y \leq 0.4$.

The composition of tetrahedrite from the Keno Hill district approximates $(\text{Cu}, \text{Ag})_{10+X}(\text{Fe}, \text{Zn}, \text{Cd})_{2+Y}(\text{Sb}, \text{As})_{4+Z}\text{S}_{13}$, where $0.8 \leq X \leq 2.1$, $0.1 \leq Y \leq 0.5$, and $0.3 \leq Z \leq 0.8$ (Table 2). As can be seen, combined Cu and Ag in particular may greatly exceed proportions quoted in the ideal formula. The high cation content is reflected in the low proportion of S, which varies from 18.32 to 22.48 wt. % (Table 1). Similar low sulfur totals and high cation contents are reported from other districts by Petruk *et al.* (1971) (20.1% S), Riley (1974) (20.4% S), Kvacek *et al.* (1975) (17.3% S), Patrick (1978) (20.5% S), Sandecki & Amcoff (1981) (19.6% S), Basu *et al.* (1981) (20.8% S), among others. These are all from Ag-rich tetrahedrite or freibergite samples and have metals and semimetals in considerable excess of the ideal formula.

The greatest elemental variations in the analyzed samples presented in Table 1 occur with Ag, Cu, Fe and Zn. The As and Sb contents, on the other hand, are surprisingly constant in light of zoning studies undertaken in other mining districts (Hackbarth &

Petersen 1984). A plot of Ag *versus* Cu displays a negative linear correlation (Fig. 8A), indicating direct substitution between Ag and Cu. The trigonal planar sites (TRG) and the tetrahedral sites (TET) are both occupied in part by Ag. Within the tetrahedrite series, the samples with high silver values (Ag > 20 wt. %) of the Keno Hill district are more correctly termed freibergite according to the limits of Riley (1974). A similar linear relation is observed between Fe and Zn in the tetrahedral sites (Fig. 8B). Iron increases from 0.4 to 2.3 atoms as zinc decreases from 1.9 to 0.1 atoms per 13 sulfur atoms. The increasing Fe/Zn and Ag/Cu values correspond to the spatial distribution of the samples in the district, matching the east-to-west or "downstream" zoning sequence.

The spatial variation in tetrahedrite chemistry is more fully displayed in Figure 9. The map shows the variation of the average Ag/(Cu + Ag) value from individual polished mounts according to position in the district. Individual samples may display considerable internal variability (Table 1); however, this variability is never as great as the district-wide trend, which shows a distinct increase in the value toward the east. The chemical zonation stands out clearly, and may suggest a strong component of lateral migration for the mineralizing fluids.

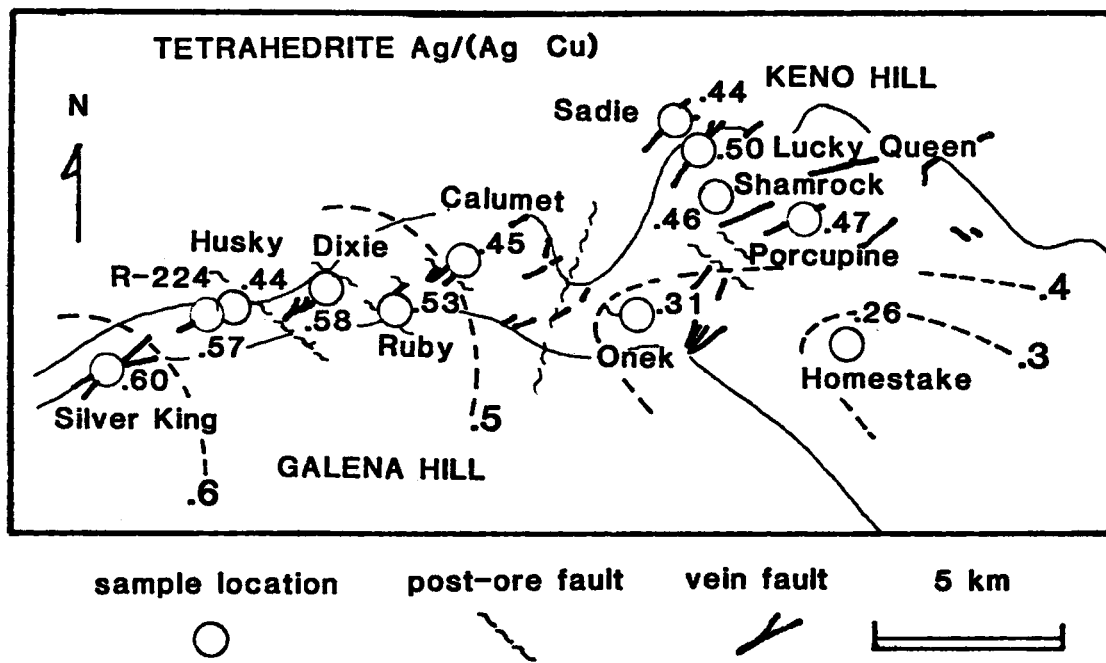


FIG. 9. Map of spatial variation in Ag/(Cu + Ag) from tetrahedrite-freibergite samples taken across the Keno Hill district. Results plotted are average values from individual polished mounts, in number of atoms relative to 13 atoms of sulfur.

DISCUSSION

The Keno Hill mining district is part of a large, zoned, fossil hydrothermal system. Mineralogical variations within individual orebodies do not generally show any obvious or systematic patterns on a detailed scale. However, regular zonation of mineral distribution is clearly developed on a district-wide scale. Consequently, the district may be viewed as a large continuous deposit formed from one com-

plex hydrothermal system. Mining activities define a multitude of individual orebodies, but the zonal patterns indicate a large uninterrupted system. This system is more completely viewed from a larger-scale perspective, allowing the formulation of a useful exploration model.

The veins are confined mainly to the Keno Hill Quartzite and extend laterally for nearly 40 km. The data imply a vast network of interconnected faults and fractures linking all sectors, during lateral flow

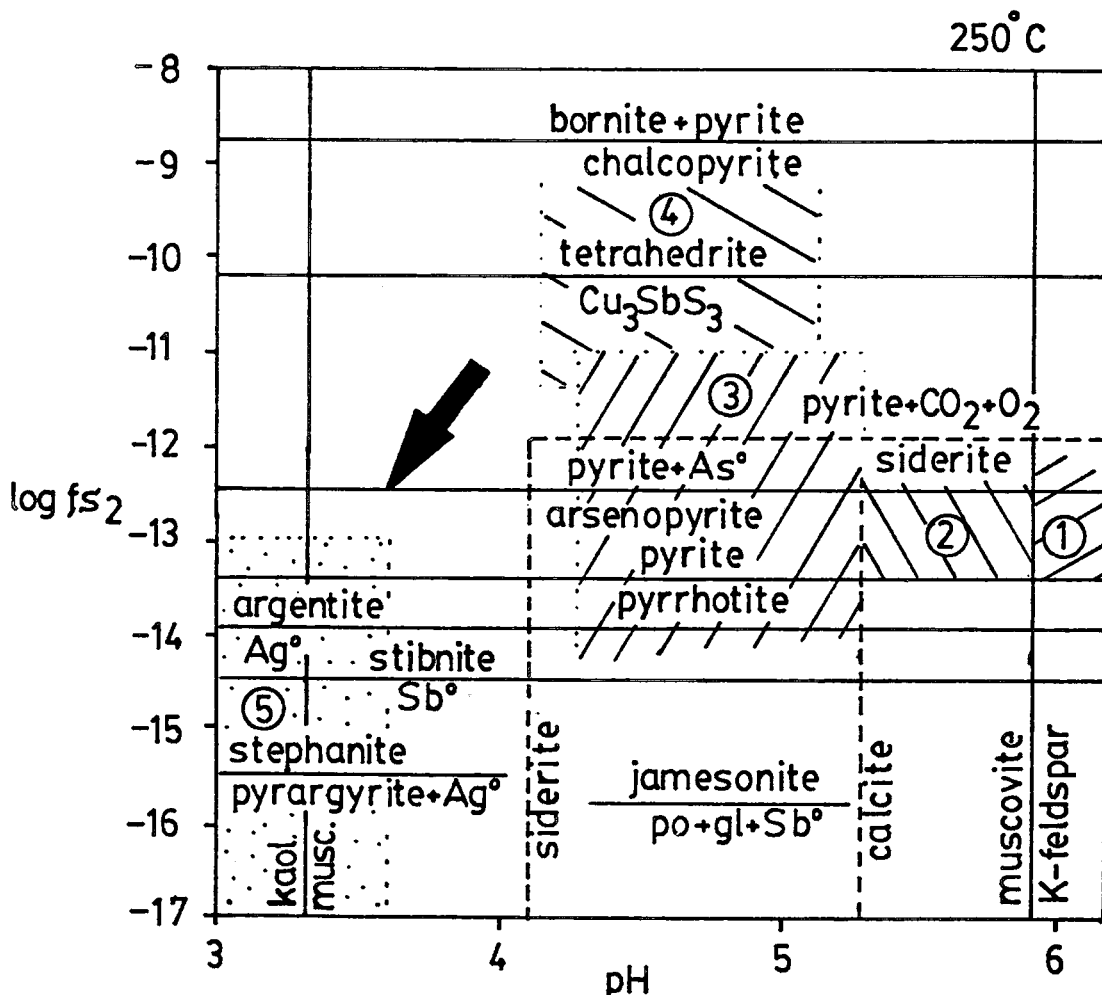


FIG. 10. A representation of the stabilities of minerals from across the various zones of the Keno Hill mining district at 250°C. The sequence 1 to 5 represents a portion of the east-to-west zonation. Parameters used for the calculations have been estimated from a fluid-inclusion study (Lynch 1989) and by analogy with other types of hydrothermal systems (Barnes 1979, Ohmoto *et al.* 1983). A value of $\log f(O_2) = -37$ was used, which is near the upper stability limit of graphite. Clathrates that form in fluid inclusions within siderite provide an estimate of the CO_2 content: $\log f(O_2) = 1.5$. Siderite saturation established the iron content ($\log \alpha(\text{Fe}^{2+}) = -4.1$), and calcium was set equal to this value in order to compare the relative effects of pH on the two types of carbonates. The activity of K^+ used is 0.05. The sources of thermodynamic data are Craig & Barton (1973) for the sulfosalts, Barton & Skinner (1979) for the sulfides, and Bowers *et al.* (1984) for the carbonates and silicates.

of fluid. Where mining activity is extensive, the continuity across mineralogical zones is clearly shown; however, limited exposure in some areas and lack of mining in the noneconomic portions of the system necessitate considerable extrapolation between other mineral zones.

The mineral sequence in the Keno Hill district offers a fairly complete example of classic zoning models (Spurr 1907, 1912, Emmons 1936). These are generally pieced together from various districts and are rarely complete in any one system. In this case, veins near the Mayo Lake Pluton are characterized by extensive quartz-feldspar veining with epidote, white mica, and some sulfides, and local Sn-

mineralization. Outward from the pluton, in the central portion of the system, Ag-Pb-Zn mineralization and carbonate gangue are present. The outermost part of the sequence has a more epithermal character, as is evident from the presence of pyrargyrite, polybasite, stephanite, acanthite and native silver wire, as well as a quartz-dominated gangue with clay alteration.

Mineralogical changes within vein deposits generally occur along the inferred direction of fluid flow. In contrast to other settings, vertical zoning at Keno Hill is less well developed than lateral zoning. The mineral distribution in the area indicates a predominantly unidirectional component of fluid

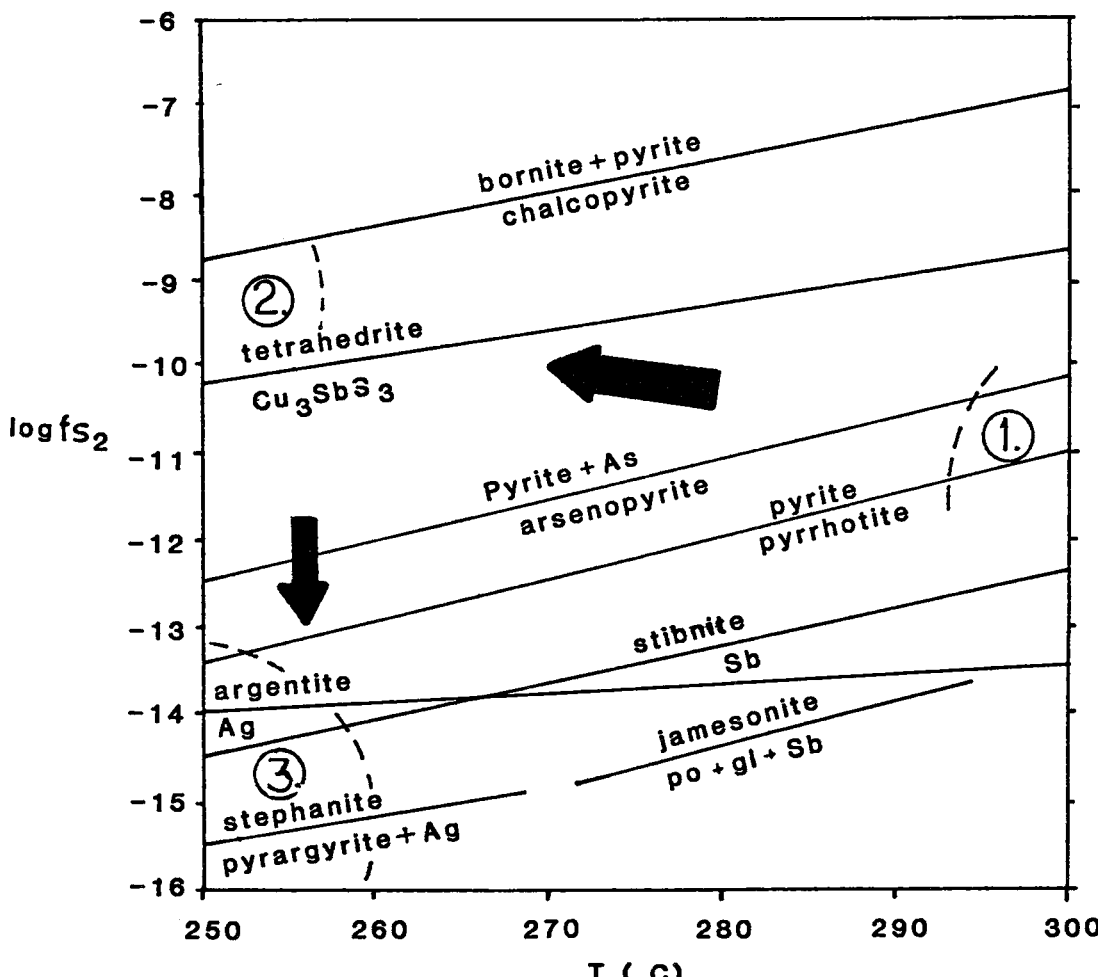


FIG. 11. Diagram illustrates early paragenesis of arsenopyrite and pyrrhotite evolving to a later tetrahedrite-bearing assemblage upon cooling at a constant sulfur fugacity. Transition may also have occurred with an increase in sulfur fugacity. Late epithermal assemblage appears to have formed from a fluid distinctly depleted in sulfur, as indicated by the presence of pyrargyrite, stephanite, native silver and argentite. Thermodynamic data are taken from Craig & Barton (1973).

migration from east to west, as controlled by favorable structures. The confinement of the hydrothermal system to the fractured quartzite provides a largely complete section of the hydrothermal system at one erosional level. The permeability and relatively nonreactive nature of the quartzite, as indicated by generally meager alteration haloes, coupled with likely moderate gradients in pressure and temperature in the lateral dimension (relative to the vertical), have allowed for the spatially extensive development of the system.

The mineralogical zones progress away from the Mayo Lake Pluton in a regular and systematic way, demonstrating a spatial relation to the pluton. However, hydrothermal veins begin outside both the pluton and its contact metamorphic aureole. The pluton remains unaltered for the most part, and no material input from the pluton to the vein system is apparent. The pluton seems to have acted only as a heat source. This idea probably explains the minor development of Sn and W mineralization relative to Ag-Pb-Zn.

In order to discuss some of the possible reasons for the mineral zoning, phase diagrams that display relevant assemblages have been prepared (Figs. 10, 11). The parameters $f(S_2)$ and pH were chosen since the mineral assemblages indicate that these were variable during hydrothermal mineralization. Oxygen fugacity, on the other hand, is considered to have been fairly constant during the principal stage of mineralization owing to the buffering capacity of graphite (French 1966). However, late-stage fluids may have been oxidized, as indicated by the presence of barite. Fluid-inclusion studies (Lynch 1989) indicate that ore formation occurred within the temperature interval 250 – 310°C.

The most obvious trend in the evolution of the hydrothermal chemistry is that of a decreasing pH from east to west, reflected by the sequence K-feldspar to muscovite to kaolinite. Also, the transition from calcite to siderite may have been due to a lowering of the pH, since for similar concentrations of Ca^{2+} and Fe^{2+} in a hydrothermal fluid, siderite is stable under more acid conditions. The increase in acidity was most likely due to the formation of carbonic acid during progressive CO_2 acquisition by the interaction of water and graphite. In the epithermal environment, acid conditions and the formation of kaolinite are often associated with boiling and the condensation of volatile phases such as CO_2 and H_2S (Knight 1977). Kaolinite in the western portion of the Keno Hill district may indicate extensive boiling in this area, and the accumulation of CO_2 .

In the ore assemblage, the presence of pyrrhotite and arsenopyrite indicate that the mineralizing fluids had a generally low sulfidation state. For tetrahedrite to have followed these in the paragenetic

sequence, a slight increase in $f(S_2)$ or decrease in temperature would have been necessary (Fig. 11). Tetrahedrite does not appear to have formed directly during the epithermal stage at the western extremity of the system, where the assemblage of native Ag, pyrargyrite, stephanite, and argentite requires sulfidation states below the stability of tetrahedrite. A low sulfidation state may have been induced either by extensive H_2S loss during boiling, or by the influx of meteoric water with a low S content, or through oxidation of H_2S to SO_4^{2-} . This last possibility is indicated by the occasional presence of barite in the epithermal assemblage.

Summary and discussion of tetrahedrite chemistry

Tetrahedrite is the dominant silver-bearing phase in the system and is distributed along the entire 25-km length of the mining district. It is present in several of the mineralogical zones. The chemistry of the tetrahedrite series is complex, but offers a more quantitative representation of the zoning and serves to corroborate zoning established by megascopic observations in the field.

In the Keno Hill district the solid solution in the tetrahedrite series varies from tetrahedrite nearer the pluton, to freibergite in the more distal assemblages. Elemental variations are characterized by substitutions between Ag and Cu, as well as between Fe and Zn. Substitution within one pair appears to be independent of substitution within the other. A high Sb/As value is observed in all samples.

The observed compositional trends are typical of tetrahedrite-bearing hydrothermal veins, with fluid evolution and differentiation interpreted to be due to fractional crystallization of tetrahedrite (Hackbart & Petersen 1984); Cu and Zn are partitioned into the mineral at an early stage and enrich the fluid in the Ag and Fe. Small-scale variations result when a mineral grows from more or less evolved fluids at different times. However, mixing of different fluids in this district seems to have been important in controlling the chemistry of the tetrahedrite series; a stable isotope study of quartz associated with tetrahedrite shows that meteoric waters were involved in the precipitation of freibergite (Lynch 1989).

Recent studies have shown that substitutions in tetrahedrite involving As-Sb, Fe-Zn and Cu-Fe may be considered ideal (Sack & Loucks 1985), but that Ag-Cu substitution is nonideal (Johnson *et al.* 1987). Problems with the general tetrahedrite formula arise in Ag-rich samples and are reported also for synthetic Cu-rich samples, for which an expanded formula is required. Makovicky & Skinner (1978) suggested, in the case of synthetic Cu-rich tetrahedrite, that the excess "mobile copper" may occupy interstitial cavities within the structure. The expanded formula seems to apply as well to the naturally occurring Ag-

rich samples of the Keno Hill district. Sandecki & Åmcoff (1981) reported on tetrahedrite samples with compositions similar to those of the Keno Hill district, in which a deficiency in sulfur or excess in cations for Ag-rich samples is recorded. They suggested that since a net surplus in charge is impossible, the cation surplus may be due to the presence of cations that are in a reduced state. This could be a possibility as well for the samples from the Keno Hill district, especially in light of the reducing nature of the graphitic host-rocks.

The low sulfidation state for the mineralizing fluids of the Keno Hill system, as indicated by the presence of pyrrhotite and arsenopyrite, would also have contributed in the formation of S-deficient tetrahedrite. Although 13 S atoms per formula unit is the most widely accepted, (Johnson *et al.* 1986), some investigators still favor a 12 S model (Babushkin *et al.* 1984).

ACKNOWLEDGEMENTS

Financial support was obtained from the Geology Division of the Northern Affairs Program, Whitehorse, Yukon, and from the Canada-Yukon Economic Development Agreement, to which I am very grateful. United Keno Hill Mines Ltd. permitted full access to their mine workings and drill core; it also provided accommodations during field work. For this help, thanks are due to chief geologist K. Watson. Invaluable assistance was provided by Steve Launspach during microprobe analysis and data processing. Substantial improvements to the article resulted from the reviews of U. Petersen, R.C. Peterson, and J.L. Jambor. Also, I thank B.E. Nesbitt for many discussions on the topic of hydrothermal zoning.

REFERENCES

- ANDERSON, R.G. (1987): Plutonic rocks of the Dawson map area, Yukon Territory. *Geol. Surv. Can., Pap. 87-1A*, 689-697.
- ANDREWS, A.J. (1986): Silver vein deposits: summary of recent research. *Can. J. Earth Sci.* **23**, 1459-1462.
- BABUSHKIN, A.N., KOBELEV, L. YA. & ZLOKAZOV, V.B. (1984): Spontaneous deformation in a single crystal of Cu_3AsS_3 . *Sov. Phys. Cryst.* **29**, 478-480.
- BARTON, P.B. & SKINNER, B.J., JR. (1979): Sulfide mineral stabilities. In *Geochemistry of Hydrothermal Ore Deposits* (H.L. Barnes, ed.). John Wiley and Sons, New York (278-403).
- BARNES, H.L. (1979): Solubilities of ore minerals. In *Geochemistry of Hydrothermal Ore Deposits* (H.L. Barnes, ed.). John Wiley and Sons, New York (404-460).
- BASU, K., BORTNYKOV, N., MOKHERJEE, A., MOZGOVA, N. & TSEPIN, A.I. (1981): Rare minerals from Rajpura-Dariba, Rajasthan, India. III. Plumbian tetrahedrite. *Neues Jahrb. Mineral., Abh.* **141**, 180-189.
- BOSTOCK, H.S. (1948), Mayo, Yukon Territory. *Geol. Surv. Can., Map 890A*.
- BOWERS, T.S., JACKSON, K.J., & HELGESON, H.C. (1984): *Equilibrium Activity Diagrams for Coexisting Minerals and Aqueous Solutions at Pressures and Temperatures to 5 kb and 600°C*. Springer Verlag, New York.
- BOYLE, R.W. (1965): Geology, geochemistry, and origin of the lead-zinc-silver deposits of the Keno Hill - Galena Hill area, Yukon Territory. *Geol. Surv. Can. Bull.* **111**.
- CRAIG, J.R. & BARTON, P.B., JR. (1973): Thermochemical approximations for sulfosalts. *Econ. Geol.* **68**, 493-506.
- EMMONS, W.H. (1936): Hypogene zoning in metalliferous lodes. *Int. Geol. Congr. 16th* **1**, 417-432.
- FRENCH, B.M. (1966): Some geological implications of equilibrium between graphite and a C-H-O gas phase at high temperatures and pressures. *Rev. Geophys.* **4**, 223-253.
- GOODWIN, C.I., SINCLAIR, A.J. & RYAN, B.D. (1982): Lead isotope models for the genesis of carbonate hosted Zn-Pb, shale-hosted Ba-Zn-Pb, and silver-rich deposits in the northern Canadian Cordillera. *Econ. Geol.* **77**, 82-94.
- GREEN, L.H. (1971): Geology of Mayo Lake, Scougale Creek and McQuesten Lake map areas, Yukon Territory. *Geol. Surv. Can. Mem.* **357**.
- GUILBERT, J.M. & PARK, C.F., JR., (1986). *The Geology of Ore Deposits*. W.H. Freeman and Co., New York.
- HACKBARTH, C.J. & PETERSEN, U. (1984): A fractional crystallization model for the deposition of argentian tetrahedrite. *Econ. Geol.* **79**, 448-460.
- JAMBOR, J.L. & LAFLAMME, J.H.G. (1978): The mineral sources of silver and their distribution in the Caribou massive sulphide deposit, Bathurst area, New Brunswick. *CANMET Rep.* **78-14**.
- JOHNSON, M.L. & BURNHAM, C.W. (1985): Crystal structure refinement of an arsenic-bearing argentian tetrahedrite. *Am. Mineral.* **70**, 165-170.
- JOHNSON, N.E., CRAIG, J.R. & RIMSTIDT, J.D. (1986): Compositional trends in tetrahedrite. *Can. Mineral.* **24**, 385-397.
- _____, _____ & _____ (1987): Effect of substitution

- on the cell dimension of tetrahedrite. *Can. Mineral.* **25**, 237-244.
- _____, ____ & ____ (1988): Crystal chemistry of tetrahedrite. *Am. Mineral.* **73**, 389-397.
- KNIGHT, J.E. (1977): A thermochemical study of alunite, enargite, luzonite, and tennantite deposits. *Econ. Geol.* **72**, 1321-1336.
- KVACEK, M., NOVAK, F. & DRABEK, M. (1975): Canfieldite and silver-rich tetrahedrite from the Kutna Hora ore district. *Neues Jahrb. Mineral., Monatsh.*, 171-179.
- LYNCH, J.V.G. (1989): *Hydrothermal Zoning in the Keno Hill Ag-Pb-Zn Vein System, Yukon: a Study in Structural Geology, Mineralogy, Fluid Inclusions, and Stable Isotope Geochemistry*. Ph.D. thesis, Univ. Alberta, Edmonton, Alberta.
- MAKOVICKY, E. & SKINNER, B.J. (1978): Studies of the sulfosalts of copper. VI. Low-temperature exsolution in synthetic tetrahedrite solid solution; $Cu_{12+x}Sb_{4+y}S_{13}$. *Can. Mineral.* **16**, 611-623.
- McTAGGART, K.C. (1960): The geology of Keno and Galena Hills, Yukon Territory. *Geol. Surv. Can. Bull.* **58**.
- MONGER, J.W.H., PRICE, R.A. & TEMPELMAN-KLUIT, D.J. (1982): Tectonic accretion and the origin of the two major metamorphic and plutonic wefts in the Canadian Cordillera. *Geology* **10**, 70-75.
- OHMOTO, H., MIZUKAMI, M., DRUMMOND, S.E., ELDIDGE, C.S., PISUTHA-ARNOND, V. & LENAGH, T.C. (1983): Chemical processes of Kuroko formation. In *The Kuroko and Related Volcanogenic Massive Sulfide Deposits* (H. Ohmoto & B.J. Skinner, Jr., eds.). *Econ. Geol. Monogr.* **5**, 570-604.
- PATRICK, R.A.D. (1978): Microprobe analysis of cadmium-rich tetrahedrites from Tyndrum, Perthshire, Scotland. *Mineral. Mag.* **42**, 286-288.
- PETRUK, W. & STAFF (1971): Characteristics of the sulphides. *Can. Mineral.* **11**, 196-231.
- POULTON, T.P. & TEMPELMAN-KLUIT, D.J. (1982): Recent discoveries of Jurassic fossils in the Lower Schist division of central Yukon. *Geol. Surv. Can., Pap.* **82-1C**, 91-94.
- RILEY, J.F. (1974): The tetrahedrite-freibergite series, with reference to the Mount Isa Pb-Zn-Ag orebody. *Miner. Deposita* **9**, 117-124.
- SACK, R.O. & LOUCKS, R.R. (1985): Thermodynamic properties of tetrahedrite-tennantites: constraints on the interdependence of the $Ag = Cu$, $Fe = Zn$, $Cu = Fe$, and $As = Sb$ exchange reactions. *Am. Mineral.* **70**, 1270-1289.
- SANDECKI, J. & ÅMCOFF, O. (1981): On the occurrence of silver-rich tetrahedrite at Garpenberg Nora, central Sweden. *Neues Jahrb. Mineral., Abh.* **141**, 324-340.
- SANGSTER, D.F. (1984): Felsic intrusion associated silver-lead-zinc veins. In *Canadian Mineral Deposit Types: a Geological Synopsis* (O.R. Eckstrand, ed.). *Geol. Surv. Can., Econ. Geol. Rep.* **36**.
- SINCLAIR, A.J., TESSARI, O.J. & HARAKAL, J.E. (1980): Age of Ag-Pb-Zn mineralization, Keno Hill - Galena Hill area, Yukon Territory. *Can. J. Earth Sci.* **17**, 1100-1103.
- SKINNER, B.J., LUCE, F.D. & MAKOVICKY, E. (1972): Studies of the sulfosalts of copper. III. Phases and phase relations in the system Cu-Sb-S. *Econ. Geol.* **67**, 924-938.
- SMITH, D.G.W. & GOLD, C.M. (1979): EDATA2: a FORTRAN 4 computer program for processing wavelength and/or energy dispersive electron microprobe analyses. *Proc. 14th Ann. Conf. Microbeam Analysis Soc.*, 271-278.
- SPURR, J.E. (1907): A theory of ore deposition. *Econ. Geol.* **2**, 781-795.
- _____, (1912): Theory of ore deposition. *Econ. Geol.* **7**, 485-492.
- TEMPELMAN-KLUIT, D.J. (1970): Stratigraphy and structure of the "Keno Hill Quartzite" in Tombstone River - Upper Klondike River map-areas, Yukon Territory (116 B/7, B/8). *Geol. Surv. Can. Bull.* **180**.
- _____, (1979): Transported cataclasite, ophiolite and granodiorite in Yukon: evidence of arc continent collision. *Geol. Surv. Can., Pap.* **79-14**.
- WATSON, K.W. (1986): Silver-lead-zinc deposits of the Keno Hill - Galena Hill area, Yukon Territory. *Yukon Geol.* **1**, 83-88.

Received April 26, 1988, revised manuscript accepted February 21, 1989.